but the W–O bonds are about 0.01 Å shorter than the Ta–O bonds. Thus, the first four electrons entering the central set of "nonbonding" orbitals enter an orbital or orbitals that are slightly bonding in character. The same general trend can be seen with the last two electrons that can enter these orbitals by comparing the bond lengths in the $[Cl_3ReOReCl_5]^{4-}$ and $[Cl_5OsOOsCl_5]^{4-}$ ions. Although the M–Cl bonds increase slightly in length, the M–O bonds become shorter by ca. 0.08 Å. The ninth and tenth total electrons may well be entering a truly nonbonding orbital, since from $[Cl_5WOWCl_5]^{4-}$ to $[Cl_5ReOReCl_5]^{4-}$ there are similar slight decreases in both the M–Cl distances and the M–O distances. The change from 9 total electrons to 10 when represented by the reduction of $[Cl_5ReOReCl_5]^{3-}$ to $[Cl_5ReOReCl_5]^{4-}$ leads to a uniform decrease of about 0.03 Å in all Re–Cl and Re–O bond lengths, which may be understood by assuming that the electron is entering an essentially nonbonding orbital but that the lowering of the mean oxidation number increases the covalent radius by about 0.03 Å.

Finally, we note that this $[Cl_5TaOTaCl_5]^{2-}$ ion must share the honor of being the first Ta^V–O–Ta^V species to be reported with a compound described in the preceding paper by Chisholm, Huffman, and Tan,[16] namely, $[TaCl_2(NMe_2)_2(HNMe_2)]_2O$. That molecule has also been structurally characterized by X-ray crystallography. It lies on a general position in the unit cell, and therefore linearity of the Ta–O–Ta group is not required. However, it is only slightly bent (174°), and the two Ta–O bond lengths are practically equal at 1.928 (6) and 1.917 (6) Å. The average, 1.922 (5) Å, is significantly longer than the Ta–O distance in $[Cl_5TaOTaCl_5]^{2-}$, 1.880 (1) Å. Another interesting difference is in the lengths of the cis and trans Ta–Cl bonds. In $[Cl_5TaOTaCl_5]^{2-}$ the trans bond is longer by 0.045 (7) Å than the cis one, whereas in Chisholm's compound the trans bonds are shorter, by about 0.10 ± 0.01 Å, than the cis bond. Both of these differences can be understood as arising from the strong tendency of the NMe_2 groups to engage in donor π bonding to the metal atoms. This tendency is greater for the NMe_2 groups than for the bridging oxygen atoms, and thus the Ta–O bonds have less π character and are longer in Chisholm's compound than in ours. Furthermore, the trans influence of the NMe_2 group is then greater than that of the oxygen atom, thus causing the cis Cl atom, which is trans to an NMe_2 group, to have a longer bond than the trans Cl atom.

Acknowledgment. We thank the Robert A. Welch Foundation (Grant No. A-494) for financial support.

Registry No. $[P(CH_3)_3C_6H_5]_2[Ta_2Cl_{10}O]$, 76880-13-2; $TaCl_5$, 7721-01-9; PMe_2Ph, 672-66-2.

Supplementary Material Available: A table of observed and calculated structure factors (5 pages). Ordering information is given on any current masthead page.

(16) Chisholm, M. H.; Huffman, J. C.; Tan, L.-S. *Inorg. Chem.*, preceding paper in this issue.

Contribution from the Department of Chemistry, Texas A&M University, College Station, Texas 77843, and Molecular Structure Corporation, College Station, Texas 77840

Further Studies of the Unusual Nature of Tris(β-cyanoethyl)phosphine: Structures of the Phosphine and the Phosphine Oxide

F. ALBERT COTTON,*[1a] DONALD J. DARENSBOURG,[1a] MICHAEL F. FREDRICH,[1a] WILLIAM H. ILSLEY,[1a] and JAN M. TROUP[1b]

Received October 31, 1980

The crystal and molecular structures of tris(β-cyanoethyl)phosphine (**1**) and the phosphine oxide (**2**) have been determined. The structure of the phosphine (**1**) was solved and refined in space group $P2_1/m$ with a = 6.812 (3) Å, b = 12.988 (7) Å, c = 5.869 (2) Å, β = 91.08 (3)°, and Z = 2. The molecules lie in mirror planes and are significantly distorted from threefold symmetry. The C–P–C angles are 106.9 (1) (twice) and 97.1 (2)° while the other dimensions that should be chemically equivalent also show discrepancies, e.g., P–C = 1.818 (5) (twice) and 1.841 (2) Å and C–N = 1.156 (3) (twice) and 1.111 (6) Å. The distortions as well as the high melting point of the phosphine are attributed to intermolecular dipole–dipole forces. The oxide (**2**) crystallizes in the hexagonal space group $R3c$ with a = 13.487 (3) Å, c = 10.166 (1) Å, and Z = 6. The structure refined smoothly to R_1 = 0.028 and R_2 = 0.037. The molecule has crystallographic 3 symmetry with P–O = 1.498 (3) Å, P–C = 1.803 (2) Å, C–C = 1.519 (3) Å, C–CN = 1.459 (3) Å, C≡N = 1.133 (3) Å, O–C–C = 112.04 (8)°, and C–P–C = 106.78 (9)°.

Introduction

For many years the unusual character of tris(β-cyanoethyl)phosphine, $P(CH_2CH_2CN)_3$ (**1**), has been recognized. Most immediately obvious, perhaps, is its stability toward oxidation by O_2, which is in sharp contrast to the easy conversion of typical trialkylphosphines to the phosphine oxides. Tris(β-cyanoethyl)phosphine, on the contrary, resembles triarylphosphines such as $P(C_6H_5)_3$ in requiring the use of stronger oxidizing reagents. It was also shown 20 years ago that it has very low basicity, more like that of $P(C_6H_5)_3$ than $P(C_2H_5)_3$, as shown by its HNP value of 679 relative to 573 for $P(C_6H_5)_3$ and 111 for $P(C_2H_5)_3$.[2] [ΔHNP stands for change in the half-neutralization potential in a type of nonaqueous titration, and ΔHNP values are an inverse measure of Lewis basicity. See ref 2 for further details.] It is also the only phosphine yet known to react with $Ni(CO)_4$ to produce a metal atom cluster compound, viz., $Ni_4(\mu\text{-}CO)_6[P(CH_2CH_2CN)_3]_4$.[3]

Spectroscopic and structural data for $(NCCH_2CH_2)_3PM(CO)_n$ complexes have recently become available and serve to broaden the base of evidence for its unusual place among the phosphines. Measurements of ν_{CO}[4,6] and ^{13}C NMR

(1) (a) Texas A&M University. (b) Molecular Structure Corp.

(2) Streuli, C. A. *Anal. Chem.* **1960**, *32*, 985.
(3) Bennett, M. J.; Cotton, F. A.; Winquist, B. H. C. *J. Am. Chem. Soc.* **1967**, *89*, 5366.
(4) Tolman, C. A. *Chem. Rev.* **1977**, *77*, 313.

0020-1669/81/1320-1869$01.25/0

Table I. Crystallographic Parameters

parameter	$OP(CH_2CH_2CN)_3$	$P(CH_2CH_2CN)_3$
space group	$R3c$	$P2_1/m$
a, Å	13.487 (3)	6.812 (3)
b, Å	13.487 (3)	12.988 (7)
c, Å	10.166 (1)	5.869 (2)
α, deg	90.0	90.00
β, deg	90.0	91.08 (3)
γ, deg	120.0	90.00
V, Å^3	1601.4 (9)	519.2 (4)
Z	6	2
fw	209.19	193.19
cryst size, mm	0.40 × 0.35 × 0.50	0.15 × 0.20 × 0.60
μ, cm^{-1}	2.342	19.912
2θ range, deg	0–55	0–115
no. data	411	738
$F_o^2 > 3\sigma(F_o^2)$	397	650
no. of variables	58	83
R_1	0.028	0.056
R_2	0.037	0.094
esd	1.233	2.435
d(calcd), g/cm^3	1.301	1.236
radiation	Mo	Cu

chemical shifts[5,6] for such complexes clearly imply that $P(CH_2CH_2CN)_3$ has π acidity higher than that of typical alkylphosphines and that this plays a significant role in its bonding to low-valent metal atoms. Structural results[6] for $(NCCH_2CH_2)_3PM(CO)_5$ (M = Cr, Mo) and several analogous $R_3PM(CO)_5$ compounds with R = C_6H_5 and C_6H_5O provide strong evidence in terms of M–P and M–CO bond lengths that **1** is akin to $(RO)_3P$ as a π acceptor, stronger than Ph_3P and far stronger than trialkylphosphines in this respect.

Another peculiar feature of $P(CH_2CH_2CN)_3$ is its high melting point (97 °C) as compared to alkylphosphines of comparable steric character, e.g., $P(C_2H_5)_3$, $P(CH_2CH_2CH_3)_3$, and $P(CH_2CH_2CH_2CH_3)_3$ which are all liquids at room temperature.

In view of all of the foregoing information on $P(CH_2CH_2CN)_3$ it was surprising that the structure of the ligand itself remained unknown. In this paper we report the X-ray crystallographic determination of the structures of both $P(CH_2CH_2CN)_3$ and its oxide $OP(CH_2CH_2CN)_3$.

Experimental Section

Colorless single crystals of $P(CH_2CH_2CN)_3$ (**1**) were obtained by dissolving the crude material in toluene under a nitrogen atmosphere and heating for 1 h. The solution was quickly filtered while hot and allowed to cool very slowly to −10 °C over a period of 2 days. Colorless single crystals of $OP(CH_2CH_2CN)_3$ (**2**) were obtained by slow evaporation after the crude material was boiled in absolute ethanol.

Crystals suitable for X-ray studies for both **1** and **2** were secured to the ends of glass fibers with epoxy cement. For **1** data were collected on a Syntex P$\bar{1}$ autodiffractometer specially equipped for protein data collection. The procedure used for data collection has been described elsewhere with the following exceptions and additions.[7] Precession photographs, used to confirm the space group, lattice constant determination, and data collection were performed at a constant temperature of 2 °C. Data were collected with use of full 1° wide ω scans. A constant scan rate of 3.0 deg/min was used for $2\theta \leq 95°$ and 2.0 deg/min for the range $95° < 2\theta \leq 115°$. The solution and refinement of the structure followed the procedure used for **2**. Statistical tests indicated the centric space group; attempted refinement in space group $P2_1$ encountered difficulties. In the case of **2**, the crystal was mounted on an Enraf-Nonius CAD-4F automatic diffractometer. The procedures used for data collection and solution and refinement of the structure have been described previously.[8] An R factor test showed that the correct polarity had been selected.

Crystallographic data and other pertinent information for the two compounds are given in Table I. For each crystal the data were corrected for Lorentz and polarization effects; because of the low μ values (see Table I) no absorption corrections were applied. Tables of structure factors are available as supplementary material.

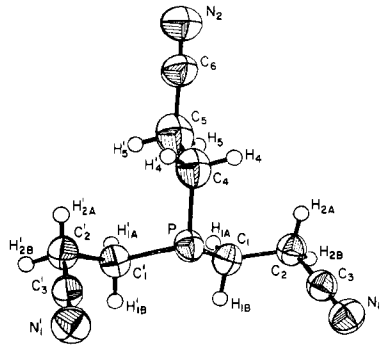

Figure 1. ORTEP view of the molecule of $P(CH_2CH_2CN)_3$ (**1**). The atoms are represented by thermal ellipsoids scaled to enclose 50% of the electron density. Hydrogen atoms are represented by arbitrarily small spheres.

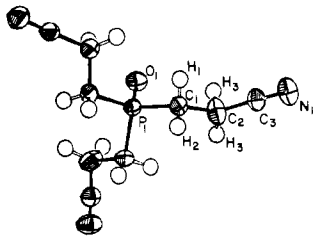

Figure 2. ORTEP view of the molecule of $OP(CH_2CH_2CN)$ (**2**). The atoms are represented by thermal ellipsoids scaled to enclose 50% of the electron density. Hydrogen atoms are represented by arbitrarily small spheres.

Results and Discussion

Final coordinates and anisotropic thermal parameters for all nonhydrogen atoms and coordinates and isotropic thermal parameters for hydrogen atoms are listed in Tables II and III for **1** and **2**, respectively. The molecular structures of **1** and **2**, seen in perspective and specified by the atomic coordinates of Tables II and III, are depicted in Figures 1 and 2. Atoms are labeled in conformity with Tables II and III, and nonhydrogen atoms are represented by ellipsoids having the shape, orientation, and relative size consistent with the thermal parameters listed for the respective atoms. Hydrogen atoms are represented by arbitrarily small spheres. Bond distances and angles are listed in Tables IV and V for **1** and **2**, respectively.

In **1** the molecules lie with the P atoms and the C_4–C_5–C_6–N_2 chain in a crystallographic mirror plane. A packing diagram of the unit cell is shown in Figure 3. The hydrogen atoms belonging to the other carbon atoms were located in an electron density difference map, and their positional and isotropic thermal parameters were successfully refined. The hydrogen atoms belonging to the carbon atoms lying in the mirror plane were not well defined and could not be refined to give realistic results. They were, therefore, introduced at calculated positions but not refined.

The results of the structural analysis of **2** reveal a crystallographic threefold axis passing through a phosphorus atom. Predictably, the coordination sphere of the phosphorus atom is a distorted tetrahedron. The O–P bond distance is 1.498 (3) Å, the O–P–C angles are 112.04 (8)°, and the C_1–P–C_1' angles are 106.78 (9)°.

(5) Bodner, G. M.; May, M. P.; McKinney, L. E. *Inorg. Chem.*, **1980**, *19*, 1951.
(6) Cotton, F. A.; Darensbourg, D. J.; Ilsley, W. H. *Inorg. Chem.* **1981**, *20*, 578.
(7) Cotton, F. A.; Frenz, B. A.; Deganello, G.; Shaver, A.; *J. Organomet. Chem.* **1973**, *50*, 227.
(8) Bino, A.; Cotton, F. A.; Fanwick, P. E. *Inorg. Chem.* **1979**, *18*, 3558.

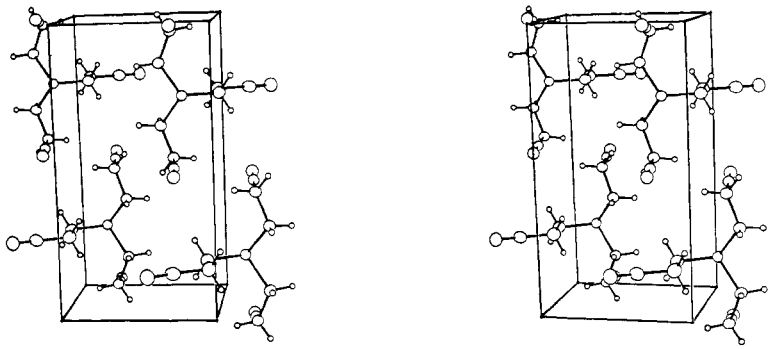

Figure 3. Stereoscopic view of the unit cell of **1**. Note the alignment of the CH_2CN groupings.

Table II. Positional and Thermal Parameters and Their Estimated Standard Deviations for $P(CH_2CH_2CN)_3$[a,b]

atom	x	y	z	B_{11}	B_{22}	B_{33}	B_{12}	B_{13}	B_{23}
P	0.2007 (2)	0.2500 (0)	0.2017 (2)	3.67 (5)	3.71 (5)	5.04 (5)	0	−0.16 (4)	0
N_1	0.2319 (5)	0.4947 (2)	−0.1784 (5)	5.6 (1)	5.5 (2)	4.5 (1)	0.0 (1)	−0.1 (1)	0.4 (1)
N_2	−0.3343 (8)	0.2500 (0)	0.8307 (9)	6.4 (2)	7.2 (3)	6.8 (2)	0	1.5 (2)	0
C_1	0.3540 (5)	0.3563 (3)	0.3121 (5)	4.5 (1)	4.1 (2)	3.9 (1)	−0.2 (1)	−0.5 (1)	0.2 (1)
C_2	0.2713 (5)	0.4631 (3)	0.2586 (6)	4.9 (1)	3.8 (1)	4.2 (1)	−0.1 (1)	−0.2 (1)	−0.2 (1)
C_3	0.2489 (5)	0.4809 (3)	0.0155 (6)	4.1 (1)	3.6 (1)	4.8 (1)	−0.2 (1)	0.2 (1)	−0.2 (1)
C_4	−0.0234 (9)	0.2500 (0)	0.3649 (10)	5.3 (3)	5.1 (2)	6.6 (3)	0	−1.0 (2)	0
C_5	0.0057 (10)	0.2500 (0)	0.6167 (12)	5.9 (3)	6.3 (3)	8.2 (3)	0	−1.3 (3)	0
C_6	−0.1960 (10)	0.2500 (0)	0.7336 (10)	8.0 (3)	5.1 (3)	6.0 (2)	0	2.8 (2)	0

atom	x	y	z	B, Å²	atom	x	y	z	B, Å²
H_{1A}	0.372 (6)	0.348 (3)	0.438 (6)	5.3 (8)	H_{2B}	0.351 (7)	0.517 (3)	0.301 (7)	6.7 (10)
H_{1B}	0.486 (5)	0.350 (2)	0.240 (5)	3.2 (6)	H_4	−0.099 (0)	0.190 (0)	0.325 (0)	5.0 (0)
H_{2A}	0.147 (4)	0.472 (3)	0.318 (5)	3.3 (6)	H_5	0.080 (0)	0.310 (0)	0.661 (0)	5.0 (0)

[a] The form of the anisotropic thermal parameter is $\exp[-1/4(B_{11}h^2a^{*2} + B_{22}k^2b^{*2} + B_{33}l^2c^{*2} + 2B_{12}hka^*b^* + 2B_{13}hla^*c^* + 2B_{23}klb^*c^*)]$.[3] [b] Estimated standard deviations in the least significant digits are shown in parentheses.

Table III. Positional and Thermal Parameters and Their Estimated Standard Deviations for $OP(CH_2CH_2CN)_3$[a,b]

atom	x	y	z	B_{11}	B_{22}	B_{33}	B_{12}	B_{13}	B_{23}
P_1	0.0000 (0)	0.0000 (0)	0.2500 (0)	2.91 (2)	2.91 (2)	2.00 (2)	$1/2B_{11}$	0	0
O_1	0.0000 (0)	0.0000 (0)	0.3974 (3)	4.4 (1)	4.4 (1)	2.02 (8)	$1/2B_{11}$	0	0
N_1	−0.3688 (2)	0.0228 (2)	0.2124 (3)	4.73 (6)	6.40 (8)	4.6 (1)	3.57 (4)	0.69 (7)	1.14 (8)
C_1	−0.1060 (2)	0.0302 (2)	0.1834 (2)	3.18 (5)	3.37 (6)	2.62 (7)	1.84 (4)	−0.13 (6)	0.12 (5)
C_2	−0.2214 (2)	−0.0445 (2)	0.2487 (3)	3.97 (7)	4.81 (7)	5.8 (1)	2.77 (5)	1.40 (8)	1.86 (8)
C_3	−0.3030 (2)	−0.0049 (2)	0.2284 (3)	3.35 (6)	4.13 (7)	3.35 (9)	1.86 (5)	0.75 (7)	0.77 (7)

atom	x	y	z	B, Å²	atom	x	y	z	B, Å²
H_1	−0.079 (2)	0.112 (2)	0.201 (3)	4.4 (7)	H_3	−0.201 (3)	−0.021 (3)	0.328 (4)	6.5 (8)
H_2	−0.112 (2)	0.020 (2)	0.088 (3)	4.7 (7)	H_4	−0.251 (2)	−0.127 (3)	0.250 (4)	9.9 (15)

[a] The form of the anisotropic thermal parameter is $\exp[-1/4(B_{11}h^2a^{*2} + B_{22}k^2b^{*2} + B_{33}l^2c^{*2} + 2B_{12}hka^*b^* + 2B_{13}hla^*c^* + 2B_{23}klb^*c^*)]$. [b] Estimated standard deviations in the least significant digits are shown in parentheses.

Table IV. Bond Distances and Angles for $P(CH_2CN_2CH)_3$

Distances, Å			
P-C_1	1.841 (2)	C_6-N_2	1.111 (6)
P-C_4	1.818 (5)	C_1-H_{1A}	0.75 (3)
C_1-C_2	1.528 (3)	C_1-H_{1B}	1.00 (2)
C_2-C_3	1.450 (3)	C_2-H_{2A}	0.93 (3)
C_4-C_5	1.486 (7)	C_2-H_{2B}	0.92 (4)
C_5-C_6	1.548 (7)	C_4-H_4	0.95 (. . .)
C_3-N_1	1.156 (3)	C_5-H_5	0.95 (. . .)
Angles, Deg			
C_1-P-C_1'	97.1 (2)	C_2-C_1-H_{1A}	113 (2)
C_1-P-C_4	106.9 (1)	C_2-C_1-H_{1B}	108 (1)
P-C_1-C_2	113.8 (2)	C_3-C_2-H_{2A}	106 (1)
P-C_4-C_5	115.2 (3)	C_3-C_2-H_{2B}	101 (2)
C_1-C_2-C_3	112.2 (2)	P-C_4H_4	108 (. . .)
C_4-C_5-C_6	109.7 (4)	C_5-C_4-H_4	108 (. . .)
C_2-C_3-N_1	179.6 (3)	C_4-C_5-H_5	109 (. . .)
C_5-C_6-N_2	175.4 (5)	C_6-C_5-H_5	109 (. . .)
P-C_1-H_{1A}	109 (2)	H_{1A}-C_1-H_{1B}	106 (3)
P-C_1-H_{1B}	107 (1)	H_{2A}-C_2-H_{2B}	110 (3)
C_1-C_2-H_{2A}	112 (2)	H_4-C_4-H_4'	109 (. . .)
C_1-C_2-H_{2B}	115 (2)	H_5-C_5-H_5'	109 (. . .)

Table V. Bond Distances and Angles for $OP(CH_2CH_2CN)_3$

Distances, Å			
P_1-O_1	1.498 (3)	C_1-H_2	0.98 (5)
P_1-C_1	1.803 (2)	C_2-C_3	1.459 (3)
N_1-C_3	1.133 (3)	C_2-H_3	0.86 (5)
C_1-C_2	1.519 (3)	C_2-H_4	0.98 (6)
C_1-H_1	0.99 (3)		
Angles, Deg			
O_1-P_1-C_1	112.04 (8)	C_1-C_2-C_3	113.9 (2)
C_1-P_1-C_1'	106.78 (9)	C_1-C_2-H_3	98 (3)
P_1-C_1-C_2	110.6 (2)	C_1-C_2-H_4	117 (3)
P_1-C_1-H_1	107 (2)	H_3-C_2-H_4	107 (4)
P_1-C_1-H_2	111 (2)	C_2-C_3-N_1	178.1 (3)
H_1-C_1-H_2	107 (2)		

The P–C and P–O bond lengths observed here are similar to those previously reported. In Ph_3PO the P–O distance is 1.483 (4) Å,[9] which may be compared with that in $OP(CH_2CH_2CN)_3$, 1.498 (3) Å. The P–C distances in the two

(9) Ruban, G.; Zabel, V. *Cryst. Struct. Commun.* **1976**, *5*, 671.

compounds described here are in the range 1.803 (2)–1.841 (2) Å, while those in $Ni_4(CO)_6[P(CH_2CH_2CN)_3]_4$[3] ran from 1.78 (3) to 1.87 (2) Å and those in $\{Ni(CN)_4[P(CH_2CH_2CN)_3]\}^{2-}$ averaged 1.833 (3) Å.[10]

The $P(CH_2CH_2CN)_3$ molecule in its crystal shows appreciable distortion from threefold symmetry. This is especially evident in the C–P–C angles, since the two crystallographically equivalent C–P–C angles are 106.9 (1)° and the third one, bisected by the mirror plane, is 97.1 (2)°. There are also other smaller but significant discrepancies between the dimensions of the two crystallographically different P–C–C–CN chains, as may be seen in Table V.

Similar distortions of the $P(CH_2CH_2CN)_3$ ligand have been observed in some, but not all, of its complexes. In $Ni_4(CO)_6[P(CH_2CH_2CN)_3]_4$ there are no significant distortions.[3] One ligand resides on a crystallographic threefold axis and has equal C–P–C angles of 100 (1)°. In the other three ligands there are small and scarcely significant variations; the three angles have the values 97 (1), 99 (1), and 100 (1)°. In the anion $\{Ni(CN)_4[P(CH_2CH_2CN)_3]\}^{2-}$, however, the three crystallographically independent angles are 99.5 (3), 105.3 (3), and 105.7 (4)°.[11] Similarly, in each of the $(OC)_5MP(CH_2CH_2CN)_3$ molecules,[6] with M = Cr, Mo, there is also a pattern of one small (ca. 99°) and two large (103–105°) angles. In these cases, the distortions could be attributed to unequal intramolecular repulsive forces arising from the incompatibility of the threefold symmetry of the $P(CH_2CH_2CN)_3$ ligand with the fourfold symmetry of the rest of the coordination sphere. It is, of course, also possible that intermolecular forces play a role.

In the case of $P(CH_2CH_2CN)_3$ itself, which should not have any inherent tendency to have unequal C–P–C angles, we believe that the distortions must arise from intermolecular forces. As mentioned in the Introduction, this compound has an unexpectedly high melting point, which is another indication that strong intermolecular forces are operating in the crystal. We suggest that these forces are mainly dipole–dipole attractions between the polar CH_2–C≡N groups. It is clear in Figure 3 that the linear, dipolar chains, C(2)–C(3)–N(1), are aligned so as to maximize dipole–dipole attractions, namely, parallel, opposite in direction and in close contact. In addition the other C–C–N units are aligned in head to head fashion so as to make additional though smaller contributions to the dipolar cohesive forces in the crystal.

It is notoriously difficult to make quantitative estimates of dipole–dipole forces in crystals, as explained, for example, by Rae,[12] in connection with crystalline HCN. We have, nevertheless, tried to obtain some quantitative idea of the magnitude of the dipole–dipole contribution to the packing energy in this case using a model in which the CH_2–C–N units are represented as acetonitrile molecules. With the assumption of point dipoles lying at the centers[13] of the CH_2CN groups, the energy contributed per interaction is given by the expression $U = -2\mu^2K/r^3$ where μ is the dipole moment[14] for acetonitrile (3.45 D), K is the Coulombic force constant (2.147×10^{11} cal·cm/C^2), and r is the distance between point dipoles. The energy of the dipole–dipole interaction for the longitudinal interaction is -1.361×10^{-20} cal or −8.198 kcal/mol while the energy for the end-on interaction is -2.813×10^{-21} cal or −1.694 kcal/mol. The sum of these energies yields a total dipole–dipole interaction energy of −9.892 kcal/mol. Whereas this value is of course a crude estimate, it is comparable to the dipole–dipole interaction energy of −6.09 kcal/mol calculated by Rae[12] for solid HCN. This dipole–dipole interaction energy might account for the unusually high melting of 95 °C for **1** and for the operation of forces strong enough to deform the C–P–C angles by 4–6° from an average of 103°. The $P(CH_2CH_2CN)_3$ ligand and low-valent metal comlexes derived from it are also extremely insoluble in noninteracting organic solvents.

Acknowledgment. We thank the Robert A. Welch Foundation (Grant No. A-494) for financial support. D.J.D. thanks Tulane University for sabbatical leave during the spring semester, 1980.

Registry No. **1**, 4023-53-4; **2**, 1439-41-4.

Supplementary Material Available: Tables of structure factors for both compounds (5 pages). Ordering information is given on any current masthead page.

(10) Foxman, B. M.; Mazurek, H. *Inorg. Chem.* **1979**, *18*, 113.
(11) These angles are not reported in ref 10. They were calculated by us using the positional parameters given in ref 10.
(12) Rae, A. I. M. *Mol. Phys.* **1969**, *16*, 257.
(13) The center of the CH_2CN fragment was calculated as the positional average of C_2, C_3, and N_1.
(14) McClellan, A. L. "Tables of Experimental Dipole Moments"; Rahara Enterprises: El Cerrito, CA, 1974; Vol. 2.